PCCP

Accepted Manuscript

ROYAL SOCIETY OF CHEMISTRY

www.rsc.org/pccp

Promoting Alkali and Alkali-Earth Metals on MgO for Enhancing CO2 Capture by First-Principles Calculation

Kiwoong Kim,[†] Jeong Woo Han,[*,‡] Kwang Soon Lee,[*,†] and Won Bo Lee[*,†]

Department of Chemical and Biomolecular Engineering, Sogang University, 35 Baekbeom-ro, Mapo-gu, Seoul 121-742, South Korea, and Department of Chemical Engineering, University of Seoul, 163 Seoulsiripdaero, Dongdaemun-gu, Seoul, 130-743, South Korea

E-mail: jwhan@uos.ac.kr; kslee@sogang.ac.kr; wblee92@sogang.ac.kr

KEYWORDS: Solid-sorbent, Metal-promoting, CO_2 capture, First-principles calculations

[*]To whom correspondence should be addressed
[†]Sogang University
[‡]University of Seoul

Abstract

Developing next-generation solid sorbents to improve the economy of pre- and post-combustion carbon capture processes has been challenging for many researchers. Magnesium oxide (MgO) is a promising sorbent because of its moderate sorption-desorption temperature and low heat of sorption. However, its low sorption capacity and thermal instability need to be improved. Various metal-promoted MgO sorbents have been experimentally developed to enhance the CO_2 sorption capacities. Nevertheless, rigorous computational studies to screen an optimal metal promoter have been limited to date. We conducted first-principles calculations to select metal promoters of MgO sorbents. Five alkali (Li-, Na-, K-, Rb-, Cs-) and 4 alkaline earth metals (Be-, Ca-, Sr-, Ba-) were chosen as a set of promoters. Compared with the CO_2 adsorption energy on pure MgO, the adsorption energy on the metal-promoted MgO sorbents is higher, except that for the Na-promoter, which indicates that metal promoting on MgO is an efficient approach to enhance the sorption capacities. Based on the stabilized binding of promoters on the MgO surface and the regenerability of sorbents, Li, Ca, and Sr were identified as adequate promoters among the 9 metals on the basis of PW91/GGA augmented with DFT+D2. The adsorption energies of CO_2 on metal-promoted MgO sorbents for Li, Ca, and Sr atoms are -1.13, -1.68, and -1.48 eV, respectively.

Introduction

To stop the progression of the greenhouse effect, the general consensus is that anthropogenic global CO_2 emission must be reduced over the next few decades. This CO_2 reduction has been mandated by worldwide associations, including the IPCC (Inter-governmental Panel on Climate Change) summit, since the first initiation of the Kyoto protocol. Therefore, capturing CO_2 from large stationary point sources, such as flue gas and syngas, has attracted the attention of many researchers.[1,2]

CCS (Carbon Capture and Sequestration) techniques have been considered a viable method to reduce the CO_2 level in the atmosphere. In CCS, chemical scrubbing with an aqueous amine-based

solvent a conventional carbon capture technique. However, recovering CO_2 from the solvent via a distillation process requires a large amount of energy for the re-boiler, where the solvent is vaporized with a large amount of water. Due to the energy-intensive regeneration step, an alternative carbon capture processes using solid sorbents has received considerable attention.[1–3] In the carbon capture process based on solid sorbents, the heat of water vaporization may be avoided by replacing the liquid solution with solid particles. Moreover, the heat capacity of the solid particles is lower than that of water.

Because of their low cost, abundance, and low toxicity, various alkali and alkaline earth metal oxides have been used as absorbents.[4] Among these absorbents, MgO is preferred due to its low heat of absorption[5] and moderate regeneration temperature (400-500 ^{o}C).[6,7] However, the practical application of MgO has been limited because of a low CO_2 sorption capacity and thermal instability during regeneration.[6] The CO_2 sorption capacity of MgO is half that of CaO.[8]

To enhance the sorption capacity, alkali metal-promoted MgO sorbents have been investigated for a decade. Lee et al.[9] developed a K_2CO_3-promoted MgO sorbent that has a CO_2 sorption capacity of 12 wt% in the presence of 9 vol% H_2O and 1 vol% CO_2 with a fast and complete regeneration. Alkali metal carbonate double salts supported on MgO, $(M_2CO_3)_n(MgCO_3)_p(MgO)_{1-p}$, where M is Li, Na, K, and Cs, were reported.[10] The maximum sorption capacity was 56 wt% in the case of Na-double salts at 375 ^{o}C and 0.7 atm CO_2 during PSA (Pressure Swing Adsorption). Xiao et al.[11] reported that a K-promoted double salt MgO sorbent had the highest sorption capacity, 8.6 wt% in a 100 % CO_2 environment. Zhang et al.[12] synthesized a Na-promoted double salt MgO sorbent, including $NaNO_3$, for CO_2 capture in the syngas of a pre-combustion process. During multiple cycle tests, the CO_2 sorption capacity was maintained at 15 wt% in a 100 % CO_2 environment. Yang et al.[13] investigated the role of $NaNO_3$ in Ca-promoted double salt and reported that $NaNO_3$ enhances the absorbent activity by facilitating ion diffusion. $NaNO_3$ on metal oxide has also been shown to act as a phase transfer catalyst in the gas-solid reaction, which increases the reaction rate and sorption capacity.[14] Liu et al.[15] developed a Cs-doped MgO based sorbent with the wet impregnation method with a maximum sorption capacity of 8.3 wt% at 300 ^{o}C. Duan et

al.[16] conducted a computational study for Na-, K-, and Ca-promoted MgO sorbents using density functional theory (DFT) and phonon dynamics. They evaluated the adequate turnover temperature of each sorbent.

Many researchers have experimentally developed metal-promoted MgO sorbents. However, to the best of our knowledge, only a few computational investigations of metal-promoted MgO sorbents for CO_2 capture have been performed. Metal promoters are also limited to a few alkali metals, such as potassium carbonate and sodium carbonate. In this study, we aimed to screen for an optimal promoter for MgO sorbents that can be used as a CO_2 absorbent based on first-principles calculations. We selected 9 metals as a set of potential promoters, including 5 alkali metals (Li-, Na-, K-, Rb-, Cs-) and 4 alkaline earth (Be-, Ca-, Sr-, Ba-) metals. The effects of the 9 metal promoters on MgO for CO_2 capture were evaluated via DFT calculations.

Computational details

Our DFT calculations were carried out with a periodic supercell model using the Vienna ab initio simulation package (VASP)[17–20] with the PW91 exchange-correlation functional.[21,22] A PAW (projector augmented wave) method[23,24] was used as a plane wave basis set with an energy cutoff of 400 eV. The long-range dispersion (van der Waals) contribution using the DFT + D2 approach of Grimme[25] was applied to all calculations. The default dispersion parameters in VASP were used, except for Cs and Ba, whose parameters were taken from Zhang et al.'s work.[26] In Venkataramanan et al's work,[27] they validated PW91/GGA provides accurate results for alkali metals over a hybrid exchange-correlation functional of MPW1PW91/6-311G(d,p). Thus, we expanded PW91/GGA augmented with DFT+D2 for alkali and alkaline earth metals. We obtained an additional set of results using an increased energy cutoff of 600 eV for Li and verified that the difference of energy cutoff of 400 and 600 eV is unaffected, which implies that the energy cutoff of 400 eV is sufficient to compare the promoters.

The defect-free MgO crystalline structure was cleaved in the (100) direction with a vacuum

region of 15 Å. Each repeated slab is composed of 5 MgO layers. The adsorbate and upper 3 layers were allowed to be relaxed, whereas the lower 2 layers were to be fixed in their bulk positions.

The adsorption energy, E_{ad}, of the metal promoter on bare MgO is defined as

$$E_{ad} = E_{P/host} - (E_P + E_{host}) \quad (1)$$

where $E_{P/host}$, E_{host}, and E_P represent the energies of the adsorption composites, host materials, and metal promoters, respectively. E_P is on the basis of the isolated atom. Lower values of E_{ad} represent a stronger adsorption of a promoter to MgO.

A Bader charge analysis was conducted using a grid-based algorithm.[28] The charge in an atom was defined as the difference between the valence charge and the Bader charge.

Results and discussion

We conducted first-principles calculations to screen candidate metal promoters (alkali metals: Li-, Na-, K-, Rb-, Cs- and alkaline earth metals: Be-, Ca-, Sr-, Ba-) for an optimal metal promoter on a MgO sorbent. First, the adsorption energies of 9 promoters on the MgO surface were calculated. CO_2 was loaded on the geometry-optimized metal-promoted MgO, and its adsorption energy was calculated and compared with the adsorption energy of CO_2 on MgO without the promoters.

Adsorption of CO_2 in Non-promoted MgO

One CO_2 molecule was adsorbed to the (3×3) surface unit cell of MgO. The adsorption energy of CO_2 on the top of the lattice oxygen was the highest among the four adsorption potential sites, i.e., the twofold bridge, fourfold hollow, on top of oxygen, and on top of magnesium.

On the top of the lattice oxygen site, the CO_2 molecule was rotated every 15^o in the vertical and horizontal direction to explore the ground state energy. Figure 1 shows the geometry-optimized structure of CO_2 adsorption on MgO. Table 1 provides the distances between the CO_2 and MgO surface atoms, CO_2 bending angle, and adsorption energy of CO_2. These structural data for the

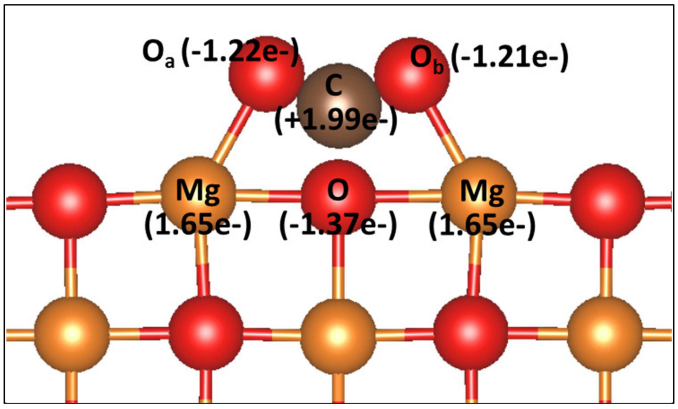

Figure 1: The optimized adsorption geometry of CO_2 on MgO surface with corresponding charge distributions; orange: magnesium, red: oxygen, brown color: carbon atoms.

fourfold hollow, twofold bridge, and the top of the lattice magnesium sites are given in the Appendix.

Table 1: The structural data of CO_2 adsorption on MgO for the top of the lattice oxygen site.

d(C-O) / Å	d(O_a-Mg) / Å	d(O_b-Mg) / Å	$\angle$ O_a-C-O_b /deg	E_{ads} / eV
1.45	2.20	2.18	133.6	-0.71

$0.43e-$ was transferred from the MgO surface to the CO_2 molecule. In this electron transfer, the largest charge transfer, $0.27e-$, was attributed to the lattice oxygen atom beneath the carbon atom.

Promotion of Alkali and Alkaline Earth Metals on MgO

The alkali and alkaline earth metals were promoted on MgO. Initially, each promoter was placed on MgO at a distance of 1.2 Å. DFT energy optimization was utilized to obtain optimized configurations of promoters on MgO, as depicted in Fig. 2.

The energy of all promoters was minimized when they are bound on top of the lattice oxygen among the MgO adsorption sites. A single promoter was adsorbed on the MgO surface unit cells of (1 $\times$ 1), (2 $\times$ 2), (3 $\times$ 3), and (4 $\times$ 4), which corresponds to an adsorption coverage of 1/2, 1/8, 1/18, and 1/32 ML (monolayer). In Fig. 3, the adsorption energies of the promoters are

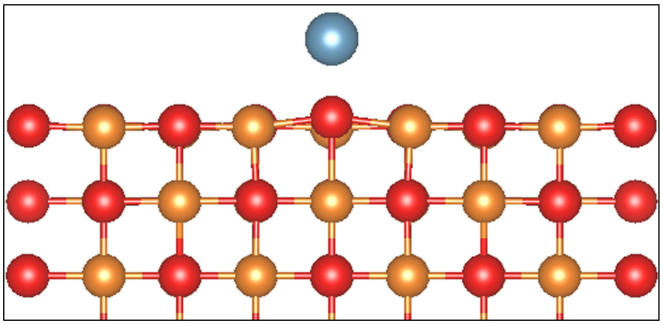

Figure 2: A side view of the relaxed structure for the promoter adsorbed on top of the lattice oxygen of MgO (3×3 surface unit cell); orange: magnesium, red: oxygen.

shown for different surface coverages. Except for the Be-promoter, 8 promoters show a similar trend: the adsorption energy negatively correlates with the surface coverage due to the repulsive force between the promoters.[29] However, at much higher coverage rates, the adsorption energies of the promoters increase again. These stabilizations were attributed to an additional cluster binding energy between the promoters, as described by Alfonso et al.[30] and Snyder et al.[31] Unlike the behaviors of the other promoters, the adsorption energy of Be continuously decreased until 1/2 ML. At a higher coverage of 1 ML, the adsorption energy of Be drastically increased to -4.39 eV. This tendency is the result of a low cohesive energy of Be, which is approximately one-third that of Ca.[32]

The distances between repeated promoters are 12.7 Åfor 1/18 ML and 17.0 Åfor 1/32 ML. To exclude horizontal interactions between adjacent promoters, we selected a surface coverage of 1/18 ML because 12.7 Åis a sufficiently long distance between promoters and less computationally taxing than 1/32 ML.

Figure 4 represents the adsorption energies of promoters at 1/18 ML with electron transfers from promoters to MgO. Because alkaline earth metals are more electronegative than alkali metals in the same row of the periodic table of the elements (PTE), alkaline earth metals more strongly adsorb to MgO than do alkali metals.

Finazzi et al.[33] adsorbed alkali metals to the MgO surface using electron paramagnetic resonance (EPR) spectroscopy and density functional theory. They concluded that the adsorption en-

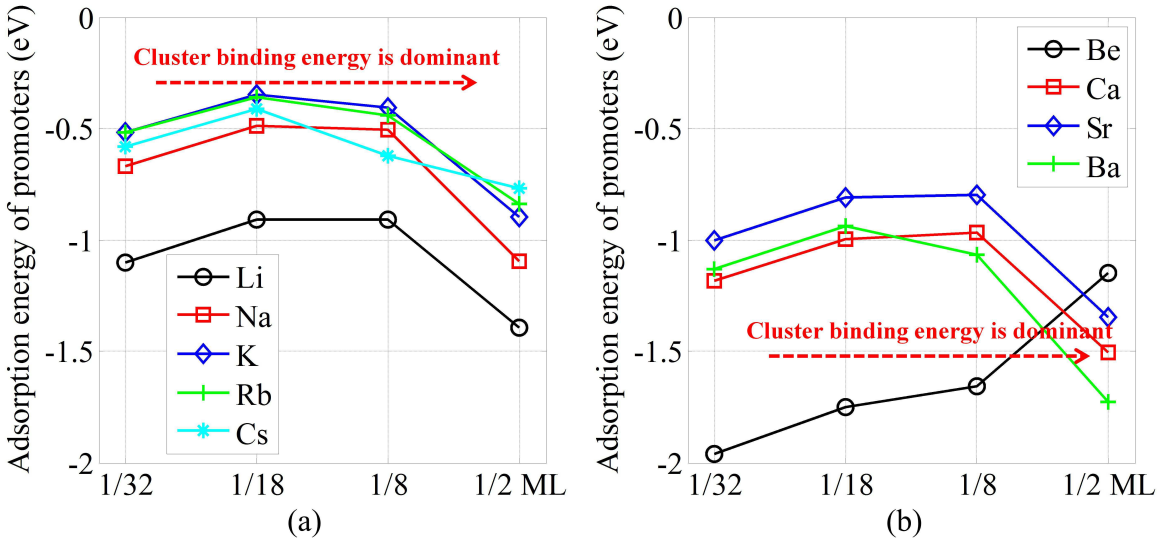

Figure 3: The adsorption energy of promoters on the MgO surface: (a) for alkali metals and (b) for alkaline earth metals.

ergies of alkali metals on MgO decrease in the following order on terrace sites: Li>Na>K. These patterns can also be observed in Fig. 4 because the electronegativity increases from the bottom to the top in PTE. Among the possible promoters the adsorption energies of Li and Be are the highest of the promoters in alkali and alkaline earth metals, whose binding is attributed to both polarization and covalent bonding with the largest charge transfer to MgO.

In general, the heat of chemisorption is greater than 0.52 eV (≈50 kJ/mol), which indicates that the cationization of alkali metals except for Li is contributed by mixed nature of physisorption and chemisorption. However, Li and alkaline earth metals are promoted on MgO via chemisorption, which more strongly stabilizes promoters.

Adsorption of CO_2 on Alkali- and Alkaline Earth Metal-Promoted MgO

CO_2 was adsorbed on alkali- and alkaline earth metal-promoted MgO to investigate effects of promoters. Figure 5 represents the adsorption energies of CO_2 of alkali- and alkaline earth metal-promoted MgO sorbents. The corresponding optimized structures and charge distributions are

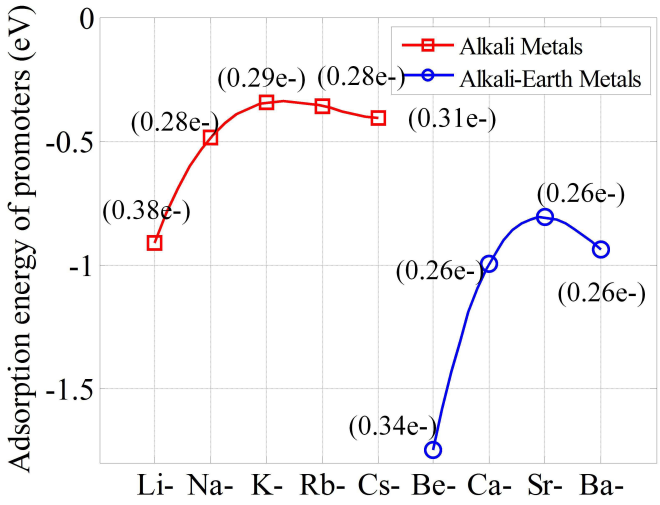

Figure 4: Adsorption energies of 9 promoters on MgO for the surface coverage, 1/18 ML. The values in parenthesis represent charge transfers from promoter to MgO.

presented in Table 2. Compared with the bending angles of CO_2 and distances of O_b-Mg and C-P for alkali metal promoters, both these angles and distances are too small for alkaline earth metal-promoted MgO. Except for the Na-promoter, the adsorption energies of CO_2 on the metal promoted MgO are higher than those on bare MgO. Similar to the highest adsorption energy found for the Li- and Be-promoter on MgO in alkali and alkaline earth metals, the adsorption energy of CO_2 was highest on Li- and Be-promoted MgO sorbents because of the high electronegativity and small Van der Waals radius, which easily transfer charge to the CO_2 molecule.

The amount of charge transferred from the MgO surface to the CO_2 molecule is $0.43e-$ in the absence of promoters, and more charge is transferred in the presence of promoters. The adsorbed CO_2 molecule becomes more negatively charged because both the promoters and the MgO in the vicinity of CO_2 donate electrons, thereby increasing the adsorption energy of CO_2. These charge transfers are very drastic for alkaline earth metal promoters due to their stronger electronegativity.

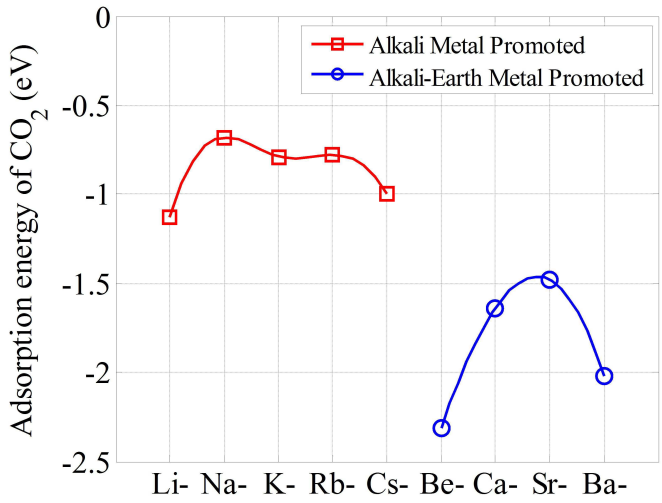

Figure 5: The adsorption energy of CO_2 on the metal-promoted MgO.

Table 2: The structural data and charge distribution of CO_2 adsorption on the metal-promoted MgO.

	P	∠ O_a-C-O_b (deg)	d(O_b-Mg) (Å)	d(C-P) (Å)	Charge distribution ($e-$)					CO_2 Ads. En. (eV)
					O_a	O_b	C	CO_2	P	
Akali Metals	Li-	136.8	2.21	2.34	-1.08	-1.23	1.43	-0.88	0.87	-1.13
	Na-	137.1	2.18	2.7	-1.11	-1.21	1.46	-0.86	0.83	-0.68
	K-	136.6	2.13	3.34	-1.00	-1.21	1.35	-0.86	0.84	-0.79
	Rb-	135.8	2.17	3.27	-1.10	-1.23	1.46	-0.87	0.84	-0.78
	Cs-	135.2	2.15	3.44	-1.14	-1.2	1.45	-0.89	0.84	-1.00
Akali-Earth Metals	Be-	122.9	2.11	1.68	-1.14	-1.24	0.78	-1.60	1.60	-2.31
	Ca-	120.9	2.10	2.36	-1.19	-1.19	0.98	-1.40	1.33	-1.68
	Sr-	121.5	2.08	2.52	-1.18	-1.22	1.00	-1.40	1.36	-1.48
	Ba-	119.3	2.09	2.69	-1.25	-1.25	1.03	-1.47	1.39	-2.02

*O_b is oxygen atom that has a shortest distance from MgO surface.

Impact of Metal Promoter on CO_2 capture

As noted in the section entitled **Promotion of Alkali and Alkaline Earth Metals on MgO**, the promoters in the top of row of PTE are more strongly adsorbed to the MgO because of their high electronegativity. However, for a metal with a large atomic radius, such as Cs and Ba, the adsorption strength increased as shown in Fig. 6, which is attributed to the attractive electrostatic interaction between Cs (or Ba) and neighboring four Mg.[34]

On the contrary, the adsorption of CO_2 is enhanced when substrates with promoters are strongly electropositive and basic, which suggests that the metals on the bottom of row of PTE are the preferred promoters for a high sorption capacity. Reddy et al.[35] reported TGA experimental results in which the CO_2 adsorption capacity was ranked as a function of the atomic radius and the basicity of the alkali metals doped on CaO, i.e., Li<Na<K<Rb<Cs. Similarly, for sodium-, potassium-, and cesium carbonate- doped MgO, the CO_2 sorption capacities were experimentally found to rank as follows: Na<K<Cs.[36] The results presented in Fig. 6 also provide the same tendency for the sorption capacities. Exceptional behaviors of Li and Be are attributed to the high cationizations of these metals, which provide a high partial charge to CO_2. Lan et al.[37] calculated the binding energy of CO_2 molecules to alkali and alkaline earth metals, and Li and Be showed much higher binding energies than did the remaining metals. These effect can be observed in Table 2, such that Li and Be are high positively charged as 0.87 and 1.60, respectively.

The complex correlations mentioned above generate the curves shown in Fig. 6. Hence, the selection of the most adequate promoter is based on two aspects: i) the stabilization of promoter binding on MgO and ii) the regenerability of CO_2. The adsorption energies of promoters must exceed 0.52 eV for stable binding on MgO to ensure thermal stability. The adsorption energy of CO_2 should be lower than 1.86 eV, which corresponds to the adsorption energy of CO_2 on CaO ($CaO + CO_2 \leftrightarrow CaCO_3$). When the adsorption energy of CO_2 exceeds 1.86 eV, the desorption would be difficult. Thus, an energy-intensive regeneration must be included, which results in a high expenditure of the process. In terms of these two aspects, we conclude that the optimal promoters are Li, Ca, and Sr on the basis of PW91/GGA augmented with DFT+D2.

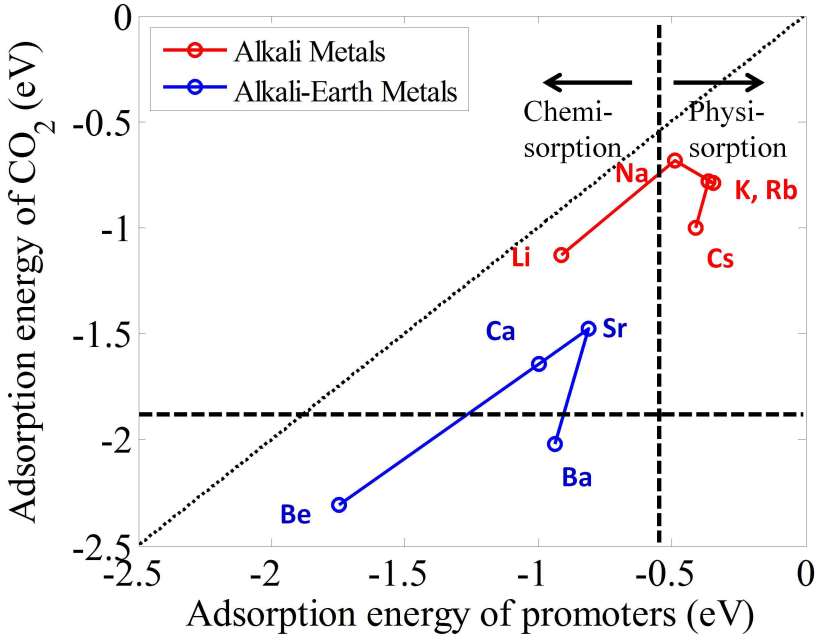

Figure 6: The adsorption energy of CO_2 on the metal-promoted MgO with respect to the adsorption energy of promoters.

To the best of the author's knowledge, Li_4SiO_4 and CaO have been utilized as high-temperature absorbents for CO_2 capture,[7] although not as a promoter. These screened metal materials (Li, Ca, and Sr) have not been used as promoters on MgO, which allows for the development of possibly improved medium temperature sorbents.

Conclusions

Overcoming the energy penalty of carbon capture processes to develop improved solid-sorbents has been a major challenge for most material-related researchers. Therefore, we screened 5 alkali metals and 4 alkaline earth metal-promoted MgO sorbents using first-principles calculations in this work. In the set of 9 alkali metal promoters, most of alkali metals, except for Li, exhibited unstable binding on MgO via mixed chemisorption and physisorption, while the other promoters, i.e., alkali earth metals and Li, showed stable binding on MgO via chemisorption. Except for the

Na-promoter, the adsorption energies of CO_2 increased compared with that on pure MgO due to promoter effects. Based on the stable promoter binding on MgO and the CO_2 regenerability, we suggest that Li-, Ca-, and Sr-promoted MgO sorbents are the most appropriate CO_2 absorbents.

The metal-promoted MgO sorbents newly proposed in this study can be connected with further MD (Molecular Dynamics) and MC (Monte Carlo) studies to investigate the dynamic diffusion and reaction behaviors and the equilibrium, as conducted by Kim et al.[3] These thermodynamic properties can be utilized as key parameters in process modeling studies to predict the bulk process performance.[1,2]

Acknowledgement

This work was supported by a grant from the Korea CCS R&D Center (KCRC), which is funded by the Korean government (Ministry of Education, Science and Technology, No. 2012-0008886), Basic Science Research Program through the National Research Foundation of Korea (NRF) funded by the Ministry of Education (2012R1A1A1042214) and the Ministry of Science, ICT & Future Planning (2014R1A1A1005303).

Appendix

Table 3: The structural data of CO_2 adsorption on MgO for the twofold bridge, fourfold bridge, and on top of the lattice magnesium sites.

	d(C-O) / Å	d(O_a-Mg) / Å	d(O_b-Mg) / Å	$\angle$ O_a-C-O_b /deg	E_{ads} / eV
Twofold bridge	2.30	2.73	2.64	163.8	-0.20
Fourfold hollow	2.86	2.58	2.66	176.6	-0.34
On top-Mg	3.55	3.24	3.33	179.3	-0.08

References

(1) Kim, K.; Kim, D.; Park, Y.-K.; Lee, K. S. *International Journal of Greenhouse Gas Control* **2014**, *26*, 135–146.

(2) Kim, K.; Son, Y.; Lee, W. B.; Lee, K. S. *International Journal of Greenhouse Gas Control* **2013**, *17*, 13–24.

(3) Kim, K.; Lee, S.; Ryu, J. H.; Lee, K. S.; Lee, W. B. *International Journal of Greenhouse Gas Control* **2013**, *19*, 350–357.

(4) Kumar, S.; Saxena, S. K. *Materials for Renewable and Sustainable Energy* **2014**, *3*, 30.

(5) Feng, B.; An, H.; Tan, E. *Energy & Fuels* **2007**, *21*, 426–434.

(6) Wang, Q.; Luo, J.; Zhong, Z.; Borgna, A. *Energy & Environmental Science* **2011**, *42*, 42–55.

(7) Choi, S.; Drese, J.; Jones, C. *ChemSusChem* **2009**, *2*, 796–854.

(8) Philipp, R.; Fujimoto, K. *The Journal of Physical Chemistry* **1992**, *96*, 9035–9038.

(9) Lee, S. C.; Chae, H. J.; Lee, S. J.; Choi, B. Y.; Yi, C.-K.; Lee, J.-B.; Ryu, C.-K.; Kim, J. C. *Environmental Science & Technology* **2008**, *42*, 2736–2741.

(10) Air Products and Chemicals, Inc., Carbon dioxide adsorbents containing magnesium oxide suitable for use at high temperatures.

(11) Xiao, G.; Singh, R.; Chaffee, A.; Webley, P. *International Journal of Greenhouse Gas Control* **2011**, *5*, 634–639.

(12) Zhang, K.; Li, X. S.; Duan, Y.; King, D. L.; Singh, P.; Li, L. *International Journal of Greenhouse Gas Control* **2013**, *12*, 351–358.

(13) Yang, X.; Zhao, L.; Xiao, Y. *Energy & Fuels* **2013**, *27*, 7645–7653.

(14) Zhang, K.; Li, X. S.; Li, W.-Z.; Rohatgi, A.; Duan, Y.; Singh, P.; Li, L.; King, D. L. *Advanced Materials Interfaces* **2014**, *1*, n/a–n/a.

(15) Liu, M.; Vogt, C.; Chaffee, A. L. *The Journal of Physical Chemistry C* **2013**, *117*, 17514–17520.

(16) Duan, Y.; Zhang, K.; Li, X. S.; King, D. L.; BBingyun, L.; Zhao, L.; Xiao, Y. *Aerosol and Air Quality Research* **2014**, *14*, 470–479.

(17) Kresse, G. *Journal of Non-Crystalline Solids* **1995**, *192*, 222–229.

(18) Kresse, G.; Hafner, J. *Physical review. B, Condensed matter* **1994**, *49*, 14251–14269.

(19) Kresse, G.; Furthmüller, J. *Computational Materials Science* **1996**, *6*, 15–50.

(20) Kresse, G. *Physical Review B* **1996**, *54*, 11169–11186.

(21) Perdew, J.; Chevary, J.; Vosko, S.; Jackson, K.; Pederson, M.; Singh, D.; Fiolhais, C. *Physical review. B, Condensed matter* **1992**, *46*, 6671–6687.

(22) Perdew, J.; Chevary, J.; Vosko, S.; Jackson, K.; Pederson, M.; Singh, D.; Fiolhais, C. *Physical review. B, Condensed matter* **1993**, *48*, 4978.

(23) Blöchl, P. E. *Physical review. B, Condensed matter* **1994**, *50*, 1545531–17979.

(24) Kresse, G.; Joubert, D. *Physical Review B (Condensed Matter and Materials Physics)* **1999**, *59*, 1758–1775.

(25) Grimme, S. *Journal of computational chemistry* **2004**, *25*, 1463–1473.

(26) Zhang, F.; Gale, J. D.; Uberuaga, B. P.; Stanek, C. R.; Marks, N. A. *Physical Review B* **2013**, *88*, 054112.

(27) Venkataramanan, N. S.; Belosludov, R. V.; Note, R.; Sahara, R.; Mizuseki, H.; Kawazoe, Y. *Chemical Physics* **2010**, *377*, 54–59.

(28) Bader, R. F. W. *Atoms in Molecules*; John Wiley & Sons, Ltd: Chichester, UK, 2002.

(29) Han, J. W.; Li, L.; Sholl, D. S. *The Journal of Physical Chemistry C* **2011**, *115*, 6870–6876.

(30) Alfonso, D.; Jaffe, J. E.; Hess, A. C.; Gutowski, M. *Surface Science* **2000**, *466*, 111–118.

(31) Snyder, J. A.; Jaffe, J. E.; Gutowski, M.; Lin, Z.; Hess, A. C. *The Journal of Chemical Physics* **2000**, *112*, 3014–3022.

(32) Mokhtari, A.; Akbarzadeh, H. *Physica B: Condensed Matter* **2003**, *337*, 122–129.

(33) Finazzi, E.; Di Valentin, C.; Pacchioni, G.; Chiesa, M.; Giamello, E.; Gao, H.; Lian, J.; Risse, T.; Freund, H.-J. *Chemistry - A European Journal* **2008**, *14*, 4404–4414.

(34) Run, X.; Gong, W.-m.; Zhang, X.; Wang, L.-j.; Hong, F. *Chinese Journal of Chemical Physics* **2010**, *5*, 538–542.

(35) Reddy, E. P.; Smirniotis, P. G. *The Journal of Physical Chemistry B* **2004**, *108*, 7794–7800.

(36) Jahan, M. *Monash University, Victoria, Australia* **2011**,

(37) Lan, J.; Cao, D.; Wang, W.; Smit, B. *ACS Nano* **2010**, *4*, 4225–4237.